ARTICLE

Cobalt Nanoparticle-Assisted Engineering of Multiwall Carbon Nanotubes

Ming-Sheng Wang,[†,*] Yoshio Bando[†] Julio A. Rodriguez-Manzo,[‡] Florian Banhart,[‡] and Dmitri Golberg[†,*]

[†]WPI Center for Materials Nanoarchitectonics (MANA), National Institute for Materials Science (NIMS), Namiki 1-1, Tsukuba, Ibaraki 305-0044, Japan, and [‡]Institut de Physique et Chimie des Matériaux, UMR 7504, Université de Strasbourg, 67034 Strasbourg, France

ABSTRACT New methods of processing multiwall carbon nanotubes (CNTs) are demonstrated in experiments in the transmission electron microscope (TEM). These include precisely controllable cutting, repairing, and interconnecting of different CNTs with the assistance of an encapsulated Co particle. All processes involve the interactions between the metal and graphitic shells that are driven by combined electrical biasing [using a scanning-tunneling microscope (STM)-TEM setup] of the CNT and focused electron-beam irradiation of a Co-containing region. In particular, we present two CNT soldering processes, that is, Co-joined and Co-catalytic connections. The former process uses a Co particle as the central node to which two CNTs are covalently attached on the opposite sides, and the latter makes use of the segregation of new graphitic shells from the metal at the connecting site, resulting in CNT plumbing. We compare the mechanical robustness of both connection types by direct force measurements in the TEM using an integrated atomic force microscope (AFM) setup. They reveal a tensile strength of 4.2 and 31 GPa, respectively, thus demonstrating the superiority of the Co-catalytic connection whose strength is already comparable to standard CNTs. In addition, all connected nanotubes show metallic conduction. The developed methods could be of particular importance in future nanoelectronic device technology.

KEYWORDS: CNT−metal interaction · CNT interconnection · tensile strength · Co-catalytic growth · TEM-STM · TEM-AFM

Carbon nanotubes (CNTs), since their identification,[1] have attracted extensive interest from scientific and industrial viewpoints owing to the richness of their mechanical and electrical properties. These are closely related to the tube geometrical features, and, therefore, controlled growth of CNTs with predefined structures is highly desirable. Catalytic chemical vapor deposition (CVD) has widely been accepted as the most controllable method of the large-scale CNT production.[2,3] During a CVD process, metal catalyst particles (*e.g.*, Fe, Ni, Co, or alloys of these) and their interactions with C atoms at a high temperature play a crucial role for determining the final morphology/atomic structure. Recently, the role played by a nanoscale catalyst during CNT growth has partly been revealed under *in situ* observation at elevated temperatures inside an environmental transmission electron microscope (TEM).[4−8] Direct observations during *in situ* TEM experiments show that the evolution of single-walled CNTs or other nanocages is strongly dependent on the catalyst size,[6] and the formation of bamboo-like structures is initiated by the particle shape evolution due to its interaction with graphitic layers.[7]

In fact, the behavior of metal nanoparticles may not only have a prominent influence on the morphology of CNTs during their growth. The interactions between a nanoparticle and graphitic structures can also be utilized to create novel CNT-based nanostructures *via* a postgrowth processes.[9−11] Taking our recent work as an example, the controlled formation of covalent heterojunctions between multiwall CNTs (MWNTs) and different metal nanocrystals (Fe, Co, Ni, and FeCo) was demonstrated *via* intense electron beam irradiation of metal-filled CNTs at temperatures of 450−700 °C.[12]

In the present work, the technique based on CNT-metal interactions at elevated temperatures and under electron beam irradiation is extended to perform the on-demand engineering of complex CNT structures. This includes precisely controllable cutting as well as repairing and interconnecting different nanotubes. Their electrical and mechanical properties are thoroughly investigated using STM and AFM holders integrated within a high-resolution transmission electron microscope. This work also gives new insight into metal−CNT interactions, which are essential for the control of CNT catalytic growth.

RESULTS AND DISCUSSION

The engineering of Co-filled CNTs, their electrical transport, and mechanical analyses were carried out using the Nanofactory

*Address correspondence to WANG.Mingsheng@nims.go.jp, GOLBERG.Dmitri@nims.go.jp.

Received for review June 16, 2009 and accepted August 4, 2009.

Published online August 13, 2009. 10.1021/nn900634f CCC: $40.75

TEM-STM[15,16] and TEM-AFM holders[17] inside a JEM-3100FEF (Jeol) field-emission TEM (Omega Filter). As seen in Figure 1, a sharp W tip was driven to contact a single Co-filled multiwall CNT protruding from the edge of a gold wire. A bias applied between the two metal electrodes was slowly increased until a Co particle began to melt and move (due to Joule heating and electromigration[18]). The corresponding voltage and current were typically 1−2 V and tens of μA, respectively. These depend on diameter, length of a CNT, and CNT/electrode contact conditions. The threshold current density for initiating the process is estimated to be ~8×10^6 A/cm^2 (see Supporting Information, Table S1 and Figure S1). For the sample in Figure 2a, the current at the melting of the Co particle (Figure 2b) was ~80 μA. An electrical bias was then immediately reduced to prevent further shrinking or moving of the particle. At this moment, the obtained *I*−*V* curves became smooth and reproducible, indicating a good and stable electrical contact due to structural annealing under biasing. The electron beam was then converged onto the particle with a current density of 500 A/cm^2 or more.

During the irradiation, the bias was maintained in order to ensure a high temperature of a tube and to prevent structural failure under electron irradiation. Then, and in line with the previously reported data,[12] a CNT−Co−CNT junction was formed (Figure 2c). This structural transformation is driven by the minimization of surface and/or interface energies and involves interdiffusion between metal and C atoms followed by final phase segregation. What should be emphasized here is that if the e-beam irradiation and biasing were still maintained, the structural transformation was still going on. As shown in Figure 2d, the Co particle becomes narrow. Figure 2e gives the structural details of a Co junction. The Co nanocrystal subsequently shrank due to Co diffusion from the junction to the left-hand CNT surface, and some new Co particles appeared (hundreds of nanometers away from the junction region, not shown here; see Figure 3d, for an analogous experiment on another tube). This phenomenon can be explained as a result of a thermally assisted electromigration process. The junction region should be the hottest point along the whole structure due to the bias-induced Joule heating of the junction that has a higher resistivity compared to other regions. This may promote the electromigration of Co atoms and therefore reduces the electrical current threshold. Once Co atoms leave the junction toward the anode (under an "electron-wind" force) and arrive at a region with a relatively low temperature, they tend to agglomerate as small particles on the outer CNT surface. Several minutes later, a narrow Co nanocrystal remains to bridge the two CNT segments (Figure 2f). Eventually it breaks (Figure 2g), with an immediate current drop to zero.

When a catalyst particle moves within the nanotube channel, it leaves a new multiwall CNT behind, as

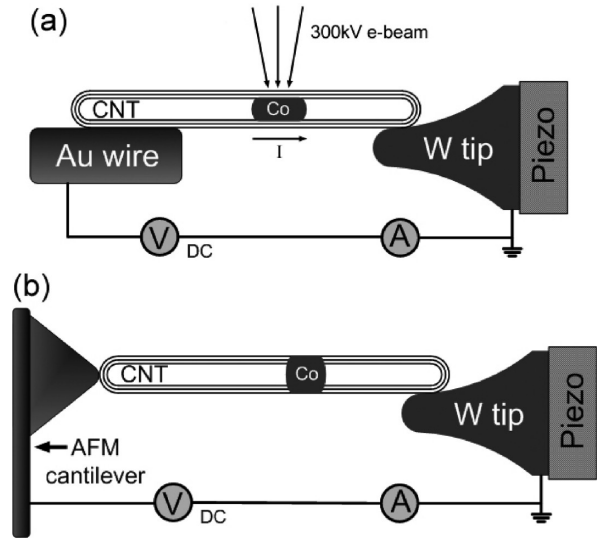

Figure 1. (a) Experimental STM setup inside the TEM. An individual Co-filled multiwall CNT protruding from the edge of a gold wire (biased) is connected to a tungsten tip (grounded). A Co particle (experiencing Joule heating) is also exposed to a focused electron beam. (b) After the formation of a CNT−Co−CNT junction, the whole structure was transferred to the AFM holder for direct force measurements inside the same TEM using a MEMS sensor.

indicated by the arrows in Figure 2b. This actually indicates that the Co particle has initially contained dissolved carbon.[19,20] Furthermore, as the Co nanocrystal (that bridges two CNT segments) shrinks, more and more graphitic shells emerge at the CNT ends (Figure 2f), which are, at least partially, due to the segregation of dissolved carbon at the CNT/Co interface (but may also be partially due to a transfer of C through the Co particle[10]). The newly formed graphitic shells tend to curl and form closed structures. This is understandable from an energetic point of view. The closed structures have a lower energy compared with the open terminals with dangling bonds. Herein, the existence of a Co particle and its interaction with the graphitic shells may actually reduce the energy for an opened CNT tip-end if it transforms to a closed one.

From another example in Figure 3, one can even more clearly see that two closed ends formed when the Co particle had vanished. Different from the case in Figure 2, the e-beam was spread over a large specimen area during the structural change from Figure 3a to Figure 3b, and the structural transformation was driven mainly under a bias increase. Finally, the original Co-filled CNT breaks into two closed-end CNTs without visible Co species on them in the field of view (Figure 3c). The Co from the former junction has been transferred to the CNT surface (hundreds of nm away) and agglomerated as small particles, see, *e.g.*, Figure 3d. The formation of two regular closed caps after cutting is a notable feature of the present method compared with pre-existing cutting techniques for MWNTs.[21,22] In addition, for the regarded process, the cutting site of a CNT can be precisely selected *via* the electromigration-

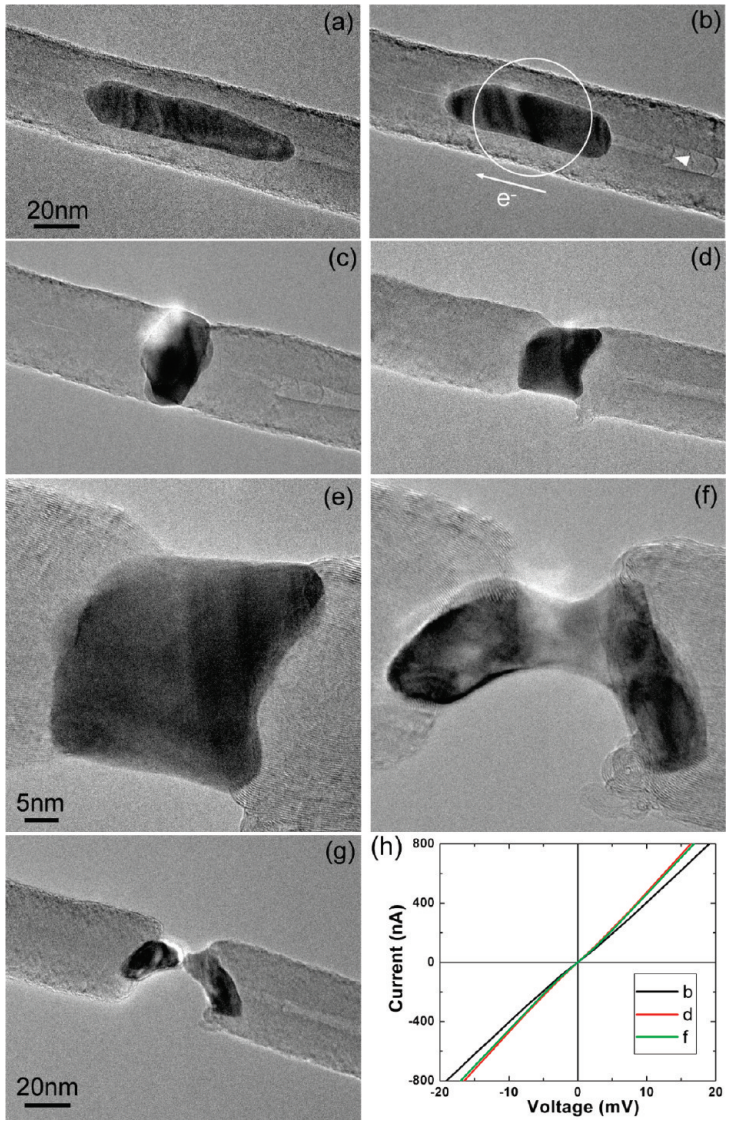

Figure 2. The Co particle encapsulated into a multiwall CNT (a) was driven to move inside the CNT by an electron flow (b). This Co-filled CNT then transforms into a CNT−Co−CNT junction under combined Joule heating and electron irradiation (focused within the encircled area) (c); the junction continues to change its morphology (d−g) under these conditions. (h) The *I*−*V* curves corresponding to the structures in panels b, d, and f.

induced motion and positioning of an encapsulated metal particle.

We also note that a Co particle-joined structure clearly shows metallic conduction. The resistance of the "joined" state was always slightly lower than the original "filled" state (see Supporting Information, Table S1, for more cases). As shown in Figure 2h, for example, the resistance in a low bias region was 23.8 kΩ in the filled state (black plot) and became 20.7 kΩ in the Co-joined state (red plot). Initially it was expected that the introduction of a metal particle between CNTs should inevitably increase the resistance of the system due to additional scattering at the junction. However, the overall transport in the present CVD-grown CNTs is diffusive (strongly affected by carrier scattering) rather than ballistic because of many defects within the tube walls. Therefore, such local interface defects would not considerablly increase the total resistance. On the other hand, the CNT−Co−CNT configuration can be considered as two CNTs in series, where a Co particle works as a connecting path. The most prominent feature of the Co particle is that it connects all concentric CNT shells directly. This may significantly increase the overall conductance of a CNT because of a short circuit between the inner and outer shells. Although the contribution from the inner shells is considerably suppressed because of the "side contact" at the two CNT ends (in which only the outermost shells directly contact the electrode) we can still find some increase in the conductance of the whole system. Interestingly, shrinking of the Co particle has almost no influence on the total resistance. For the structure in Figure 2f, the corresponding resistance is 21.3 kΩ—a very marginal increase compared with the structure in Figure 2d,e. Careful examination of the junction in Figure 2f shows that, even for a very narrow Co particle, it still contacts nearly all shells of the merged CNTs. This indicates that the contact conditions are more important, whereas the resistance of the Co particle itself is negligible. Other possible explanations for the reduction of the resistance, such as the enhancement of the electrical contact owing to Co atom diffusion from the junction to CNT/electrode contact regions, were not taken into account after careful examination of the contact areas.

Thus, the metal-filled CNT can be cut in a controlled manner.

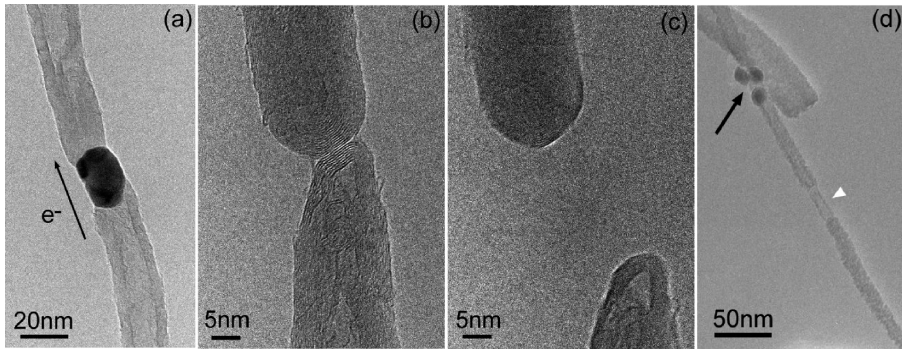

Figure 3. A CNT−Co−CNT junction (a) transforms into a CNT−CNT junction (b) when the Co particle is driven to leave the junction by an electrical current and to move along one of the tube segments. The junction was finally broken into two separate, closed CNTs. (d) Analogous experiment on another tube, displaying that the Co species originating from the junction region were transferred upward and agglomerated as small particles at the surface of the upper CNT, as indicated by an arrow. A white arrowhead points out a junction formed in this case.

Also, broken CNTs can be repaired using the metal−CNT interactions. Figure 4 gives such an example. After the original Co-filled CNT (Figure 4a) was cut *via* the above-described process in Figure 2, there still remain considerable particle fragments in the CNT channels on both sides. These two broken CNTs with Co particles at the tips were then brought into contact again by a mechanical manipulation of the piezo-driven tips (Figure 4b). A fast voltage sweep of 0−2 V was applied to this structure. The arrow in Figure 4b indicates the direction of electron flow. Consequently, the Co particle within the CNT **2** moves across the gap between the two CNTs, fuses together with the particle inside CNT **1**, and then the aggregate rapidly moves toward the anode within CNT **1** under a current flow. As a result of such particle movement, the two CNTs merge to form one, that is, the cut tube can be repaired in such a way. It should be noted here that an applied voltage sweep must be fast (within less than 1 s), otherwise, the Co particle may shrink and vanish due to continuous Co diffusion (like the case of Figure 3), instead of its movement as a whole.

It is known that a Co particle is an effective catalyst for CNT growth. Carbon atoms from the surrounding shells may dissolve in such a particle and then segregate as new graphitic structures. This process would continuously take place during the particle movement along a tube channel (as shown in Figure 2b). In the case of Figure 4, when the Co particles inside two CNTs merge at the gap, the segregation of the graphitic shells surrounding the particle may partially repair the defects near the gap. At the same time, we also notice that the graphitization of the walls of CNT **1** is largely improved after the particle has moved through this region, leaving behind a clear empty channel inside CNT **1.**

The technique to create CNT−metal−CNT junctions can also be utilized to connect chemically different nanotubes. As shown in Figure 5, a CNT−Co−CN_xNT heterojunction (CN_x, a N-doped CNT; $x < 0.1$) was created *via in situ* manipulation in TEM. We first cut a bamboo-like N-doped CNT by running through it a large current (Figure 5a).[16] The broken segment that is attached to the W tip was moved to contact an undoped CNT with a Co particle at its tip, forming an end-to-end connection (Figure 5b). The Co particle encapsulated at the CNT was then heated by passing an increasing current through the junction. The electron flow direction is from the filled CNT to the unfilled CN_xNT, as indicated by the arrows in Figure 5c. When the Co particle began to melt under Joule heating, the electron beam was quickly converged on the junction, as indicated by a white circle. It is known that intense electron irradiation can cause CNT shells to collapse,[23] and promote the process by which carbon atoms from the shells dissolve in an encapsulated Co particle.[10] The Co particle then passed across the

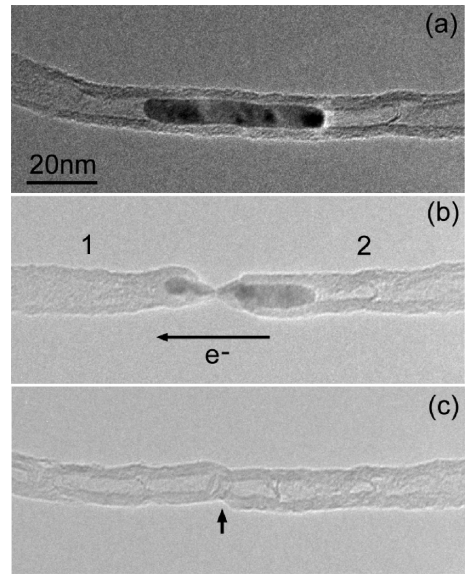

Figure 4. An originally Co-filled CNT (a) is cut by a process similar to the case presented in Figure 2. The two broken segments, each with a Co particle at the tip, are brought in contact (b) and reconnected (c). The Co particle migrated, driven by electromigration under a current flow, toward the left-hand segment of the tube. The arrow in panel c indicates the connecting site.

surrounding graphitic shells (Figure 5c), and finally penetrated into the cap of the CN_xNT (Figure 5d). As a result of such movement, the two tubes are connected *via* the central Co node. The further electrical measurement on this junction shows decent metallic conduction similar to those of the pure CNT−Co−CNT junctions, but not a rectifying diode behavior, as recorded on some other CNT/CN_xNT junctions.[24]

The above-discussed cases of Figures 4 and 5 have pointed out the two possible ways to solder CNTs. In the former case, two fragments of a cut CNT are reconnected due to an exchange of carbon atoms between a Co particle and graphitic shells, or more precisely, due to the segregation of new graphitic layers from the particle at the connecting site. It is actually a sort of catalytic behavior, and, for the sake of simplicity, we denote it a 'Co-catalytic' connection because the Co particle vanishes after having established the connection. For the latter one, two nanotubes are joined *via* a Co node that remains at the junction, and we denote it a 'Co-joined' connection. The main difference between the two connections is that in the former case, the tubes are connected *via* C−C bonds, whereas for the latter one *via* Co−C bonds.

It is of special interest to compare the mechanical robustness of the connections *via* the described two methods. This was accomplished by direct *in situ* force measurements inside the TEM. We first created a CNT−Co−CNT junction from a single Co-filled CNT *via* the process mentioned above (*i.e.*, Co-joined connection) using the STM-TEM holder. This junction, attached to the W tip, was then transferred to the AFM-TEM

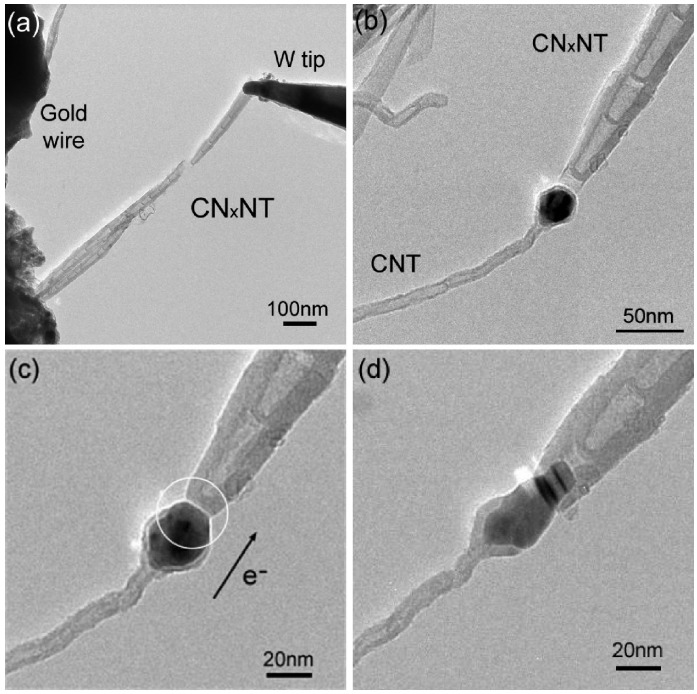

Figure 5. A series of TEM images showing the Co-mediated plumbing of a multiwall CNT and N-doped CNT (bamboo-like). (a) First a CN_xNT ($x < 0.1$) was cut by passing a large current through it. After establishing the end-to-end physical contact with a CNT having a Co particle at its tip (b), the Co particle was driven across the surrounding graphitic shells under combined Joule-heating and focused e-beam irradiation (c). Finally it penetrated into the cap of the CN_xNT and remained there (d), soldering the two tubes together. The arrow in (c) indicates the electron flow direction, and a white circle shows the focused e-beam area.

holder to measure the tensile strength inside the same TEM. As shown in Figure 6a, the junction was driven to contact a conductive AFM cantilever, which is made of Si and coated with a ~15 nm layer of Pt. To reliably evaluate the tensile strength of a junction under stretching, a stable contact of its two ends to the opposite clamps is needed. To achieve such a contact we focused an e-beam onto the two CNT ends: between the tube and the W tip, and between the tube and the W ball on the other side (attached to the AFM cantilever as a pin side). The procedure notably enhanced the adhesion forces due to a structural welding. During the force measurements, the W tip moved backward (as indicated by a black arrow in Figure 6a), and then reverted to the starting position ($Z = 0$) automatically. At the same time, the displacement of the W tip and the corresponding force (detected by the AFM MEMS sensor) were recorded. During a loading cycle with a displacement range of 500 nm, the junction was stretched and fractured at the CNT **2**/Co interface (Figure 6c). As seen on the force−displacement ($F-D$) curve (black line, with a noise level of <5 nN) in Figure 6i, the breaking force was 642 nN.

Then, for comparison, the two cut CNT fragments were joined again *via* the Co-catalytic connection by using the procedure described in Figure 4. The tubes were first brought into a physical contact (Figure 6d). We then applied a bias of −1 V on the cantilever, forcing the particle to move to CNT **2** not far from the junction region (Figure 6e). To further improve the quality of the junction, the polarity of the bias was reversed by applying +2 V on the cantilever, and the particle very quickly passed across the junction into the CNT **1** channel (in less than 1 s, see Supporting Information, Movie S1), and finally arrived at the CNT **1**/W contact (see Supporting Information, Figure S3). From the final structure of the junction (Figure 6f,g), one can see a newly formed five-shelled C capsule at the junction, bridging CNT **1** and CNT **2**. A similar force measurement was applied to such a repaired tubular structure. Under a maximum tensile load of 1371 nN (red line in Figure 6i), the junction broke at the position of the thinnest wall in the middle of the tube (Figure 6h) (see Supporting Information, Movie S2, for the whole force measurement procedure). It is noted here that a structural failure occurred at the junction, but not at the CNT−W side contacts (through a dispatch) due to much larger contact areas of these prewelded joints compared with the small Co−C contact area or cross-sectional area of the connecting CNT at the junction.

From the direct comparison of the $F-D$ curves in Figure 6i, one can see that the catalytically repaired CNT can sustain a tensile load more than twice of that for the Co-joined CNT, although the latter has a larger cross-sectional area at the junction site. In fact, the end of CNT **2** at the Co-joined junction is 14 nm in diameter (Figure 6b), and the critical strength of Co/CNT **2** junction is estimated to be 4.2 GPa, a surprisingly high value. This value is consistent with our previous results, that is, ~1−5 GPa,[25] and the latter is already comparable to carbon fibers, that is, ~5 GPa.[26] This could be an evidence of the existence of covalent bonds between carbon and metal.[12] Nevertheless, this strength is lower than that of the catalytically repaired CNT. As shown in Figure 6g, the middle five-shelled capsule has an outer diameter of 10 nm and an inner diameter of 6.6 nm, and the corresponding critical strength is calculated to be 31 GPa, more than 7 times higher than in case of the Co-joined connection. This value agrees well with the results of other tensile probing of multiwall CNTs, that yielded an ultimate strength ranging from 11 to 63 GPa.[27] This actually indicates that the repaired CNT (after having been cut) has fully recovered to the mechanical strength of an original not-fragmented CNT. In addition, different from other experiments where the MWNTs typically broke at the outermost layer (sword-in-sheath failure), in the present case, all five CNT shells of the middle thin tube were simultaneously broken, as revealed by HRTEM. That is probably because the defects within the shells increased the interlayer interactions through interlinking.[28] As a result, all CNT shells are stressed as a whole and broke at the same time.

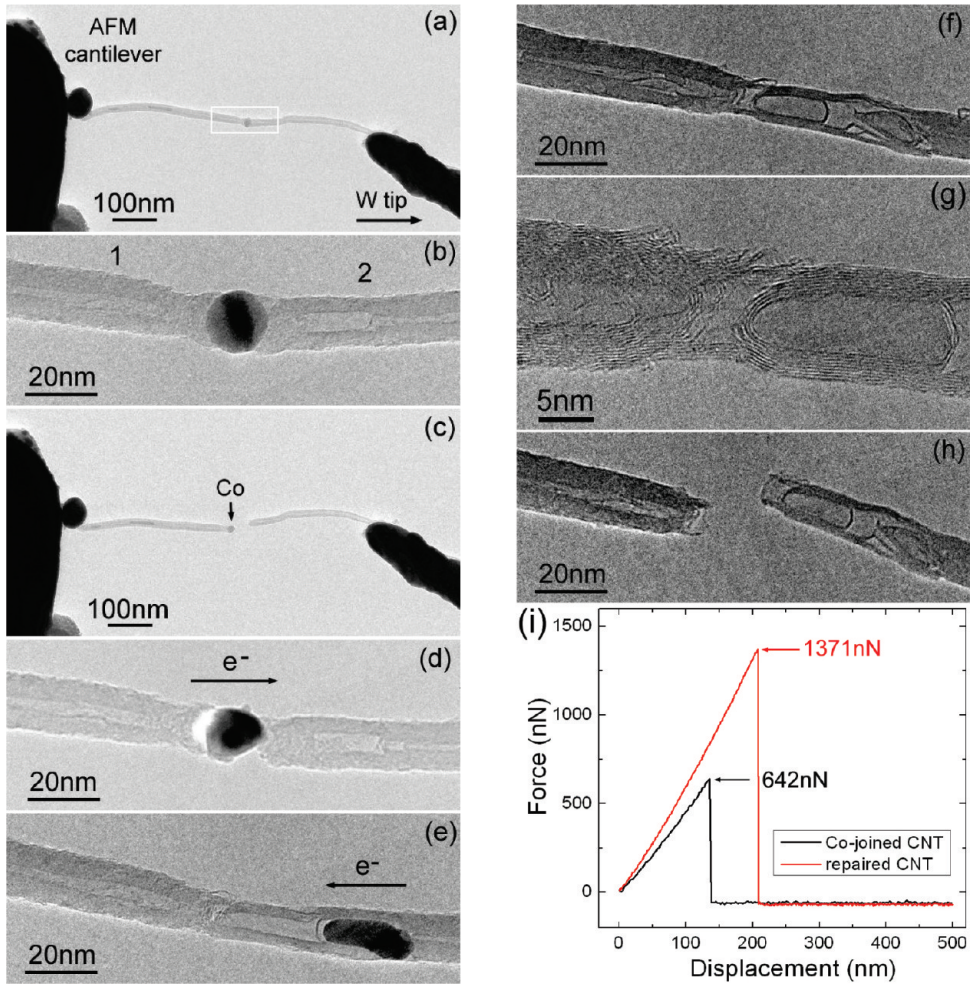

Figure 6. Comparison of the tensile strength between the Co-joined and the Co-catalytic connections by direct force measurements in the TEM using the AFM-TEM holder. (a,b) Initial linear CNT−Co−CNT junction, bridging an AFM cantilever (through the W ball attached) and a W tip; panel b shows an enlarged view of the framed area in panel a, and (c) its rupture after retraction of the W tip. The broken junction was repaired *via* the forward−backward motion of a Co particle within the tube channels (under bias polarity change), as indicated by the arrows in panels d and e; (f,g) the repaired CNT after the Co-catalytic reconnection; panel g illustrates the enlarged view of panel f; (h) the broken junction region after tensile loading. Force−displacement curves corresponding to the two types of connections (i); *i.e.*, Co-particle-joined in panels a and b and Co-particle-repaired in panels f and g.

CONCLUSIONS

To sum up, novel processing routes of individual metal-filled multiwall CNTs were designed and *in situ* tested inside a TEM. The processes involve a structural change at the metal/CNT interface that is driven by running an electrical current through the structure, combined with a focused and intense electron beam irradiation. Co-filled CNTs can be transformed into two-terminal CNT−Co−CNT junctions and then be cut precisely at the designated points of particle location. The broken CNTs may also be joined again under the electromigration-induced movement of a Co particle inside the tubes. Chemically different nanotubes, for example, CNTs and nitrogen-doped (CN_x) NTs, can also be connected to form Co-joined heterojunctions possessing decent transport properties (as documented using a STM-TEM setup). Finally, we compare the mechanical properties of Co-joined and Co-catalytic connections *via* direct force measurements in an electron microscope by using a conductive AFM-TEM setup. The resulting junctions had a tensile strength of 4.2 and 31 GPa, respectively, proving that the latter connection is more robust. All the developed processing methods are envisaged to find applications in a smart design of future CNT-based nanoelectronic circuits and devices.

METHODS

Co-filled multiwall nanotubes were synthesized by aerosol pyrolysis. Two-terminal Co-junctions were first prepared using a STM-TEM technique, as discussed in recent publications.[12−14] Further manipulations, for example, cutting, repairing, and rejoining of the CNTs using Co nanoparticles, electrical, and mechanical property measurements were conducted with the Nanofactory TEM-STM[15,16] and TEM-AFM holders[17] inside a JEM-

3100FEF field-emission transmission electron microscope (Omega Filter). Various types of junctions (attached to sharp tungsten tips) made using the STM-TEM setup were transported into the AFM-TEM holder and tensile tested under the backward piezo-moves within a displacement range of 100−600 nm. Force values were directly recorded using a MEMS sensor of the AFM cantilever. Before the mechanical measurements, the force-displacement (*F*−*D*) curves (the C values, mV/mN) were calibrated by pushing blank W tips toward a W cantilever. To improve the contact adhesion between the nanostructures and the mechanical clamps (the W cantilever and movable W tip) under tension the contact areas were irradiated with a focused electron beam ~500 A/cm^2 or more. This led to a sort of nanosoldering at the structure ends. Experimental videos were obtained by recording sequential TEM images using a CCD camera with a rate of 1−2 frame/s.

Acknowledgment. The authors would like to thank Drs. M. Mitome and Pedro M. F. J. Costa for technical support and helpful discussion in the course of this work. This work was supported by the World Premier International Center for Materials Nanoarchitectonics (MANA) of NIMS and the Deutsche Forschungsgemeinschaft (Ba 1884/6-1).

Supporting Information Available: A table presenting the detailed parameters relevant to the structural transformation of C-filled multiwall tubes into Co-joint tubes; TEM images showing the details of the interactions between CNTs and Co particles under a current flow; videos (AVI) displaying the processes of the catalytic connection establishment and a loading−unloading tensile cycle in the AFM-TEM. This material is available free of charge *via* the Internet at http://pubs.acs.org.

REFERENCES AND NOTES

1. Iijima, S. Helical Microtubules of Graphitic Carbon. *Nature* **1991**, *354*, 56–58.
2. Cassell, A. M.; Raymakers, J. A.; Kong, J.; Dai, H. J. Large Scale CVD Synthesis of Single-Walled Carbon Nanotubes. *J. Phys. Chem. B* **1999**, *103*, 6484–6492.
3. Hata, K.; Futaba, D. N.; Mizuno, K.; Namai, T.; Yumura, M.; Iijima, S. Water-Assisted Highly Efficient Synthesis of Impurity-free Single-Walled Carbon Nanotubes. *Science* **2004**, *306*, 1362–1364.
4. Helveg, S.; Lopez-Cartes, C.; Sehested, J.; Hansen, P. L.; Clausen, B. S.; Rostrup-Nielsen, J. R.; Abild-Pedersen, F; Norskov, J. K. Atomic-Scale Imaging of Carbon Nanofibre Growth. *Nature* **2004**, *427*, 426–429.
5. Sharma, R.; Iqbal, Z. *In-Situ* Observations of Carbon Nanotube Formation Using Environmental Transmission Electron Microscopy. *Appl. Phys. Lett.* **2004**, *84*, 990–992.
6. Lin, M.; Tan, J. P. Y.; Boothroyd, C.; Loh, K. P.; Tok, E. S.; Foo, Y. L. Direct Observation of Single-Walled Carbon Nanotube Growth at the Atomistic Scale. *Nano Lett.* **2006**, *6*, 449–452.
7. Lin, M.; Tan, J. P. Y.; Boothroyd, C.; Loh, K. P.; Tok, E. S.; Foo, Y. L. Dynamical Observation of Bamboo-like Carbon Nanotube Growth. *Nano Lett.* **2007**, *7*, 2234–2238.
8. Yoshida, H.; Takeda, S.; Uchiyama, T.; Kohno, H.; Homma, Y. Atomic-Scale *in-Situ* Observation of Carbon Nanotube Growth from Solid State Iron Carbide Nanoparticles. *Nano Lett.* **2008**, *8*, 2082–2086.
9. Regan, B. C.; Aloni, S.; Jensen, K.; Ritchie, R. O.; Zettl, A. Nanocrystal-Powered Nanomotor. *Nano Lett.* **2005**, *5*, 1730–1733.
10. Rodriguez-Manzo, J. A.; Terrones, M.; Terrones, H.; Kroto, H. W.; Sun, L. T.; Banhart, F. *In-Situ* Nucleation of Carbon Nanotubes by the Injection of Carbon Atoms into Metal Particles. *Nat. Nanotechnol.* **2007**, *2*, 307–311.
11. Jin, C. H.; Suenaga, K.; Iijima, S. Plumbing Carbon Nanotubes. *Nat. Nanotechnol.* **2008**, *3*, 17–21.
12. Rodríguez-Manzo, J. A.; Banhart, F.; Terrones, M.; Terrones, H.; Grobert, N.; Ajayan, P. M.; Sumpter, B. G.; Meunier, V.; Wang, M. S.; Bando, Y.; *et al*. Heterojunctions between Metals and Carbon Nanotubes as Ultimate Nanocontacts. *Proc. Natl. Acad. Sci. U.S.A.* **2009**, *106*, 4591–4595.
13. Kamalakaran, R.; Terrones, M.; Seeger, T.; Kohler-Redlich, P.; Rühle, M.; Kim, Y. A.; Hayashi, T.; Endo, M. Synthesis of Thick and Crystalline Nanotube Arrays by Spray Pyrolysis. *Appl. Phys. Lett.* **2000**, *77*, 3385–3387.
14. Elias, A. L.; Rodriguez-Manzo, J. A.; McCartney, M. R.; Golberg, D.; Zamudio, A.; Baltazar, S. E.; Lopez-Urias, F.; Munoz-Sandoval, E.; Gu, L.; Tang, C. C.; *et al*. Production and Characterization of Single-Crystal FeCo Nanowires inside Carbon Nanotubes. *Nano Lett.* **2005**, *5*, 467–472.
15. Golberg, D.; Mitome, M.; Kurashima, K.; Zhi, C. Y.; Tang, C. C.; Bando, Y.; Lourie, O.; *et al*. *In-Situ* Electrical Probing and Bias-Mediated Manipulation of Dielectric Nanotubes in a High-Resolution Transmission Electron Microscope. *Appl. Phys. Lett.* **2006**, *88*, 123101.
16. Wang, M. S.; Wang, J. Y.; Chen, Q.; Peng, L. M. Fabrication and Electrical and Mechanical Properties of Carbon Nanotube Interconnections. *Adv. Funct. Mater.* **2005**, *15*, 1825–1831.
17. Golberg, D.; Costa, Pedro M. F. J.; Lourie, O.; Mitome, M.; Bai, X. D.; Kurashima, K.; Zhi, C. Y.; Tang, C. C.; Bando, Y. Direct Force Measurements and Kinking under Elastic Deformation of Individual Multiwalled Boron Nitride Nanotubes. *Nano Lett.* **2007**, *7*, 2146–2151.
18. Svensson, K.; Olin, H.; Olsson, E. Nanopipettes for Metal Transport. *Phys. Rev. Lett.* **2004**, *93*, 145901.
19. Jensen, K.; Mickelson, W.; Han, W.; Zettl, A. Current-Controlled Nanotube Growth and Zone Refinement. *Appl. Phys. Lett.* **2005**, *86*, 173107.
20. Hansen, M. Elliott, R. P. Shunk, F. A. Institute, I. R. *Constitution of Binary Alloys*; Metallurgy and Metallurgical Engineering Series, 2nd ed; McGraw-Hill: New York, 1958.
21. Yuzvinsky, T. D.; Fennimore, A. M.; Mickelson, W.; Esquivias, C.; Zettl, A. Precision Cutting of Nanotubes with a Low-Energy Electron Beam. *Appl. Phys. Lett.* **2005**, *86*, 053109.
22. Wei, X. L.; Chen, Q.; Liu, Y.; Peng, L. M. Cutting and Sharpening Carbon Nanotubes Using a Carbon Nanotube 'Nanoknife'. *Nanotechnology* **2007**, *18*, 185503.
23. Banhart, F. Irradiation Effects in Carbon Nanostructures. *Rep. Prog. Phys.* **1999**, *62*, 1181–1221.
24. Hu, P. A.; Xiao, K.; Liu, Y. Q.; Yu, G.; Wang, X. B.; Fu, L.; Cui, G. L.; Zhu, D. B. Multiwall Nanotubes with Intramolecular Junctions (CN_x/C): Preparation, Rectification, Logic Gates, and Application. *Appl. Phys. Lett.* **2004**, *84*, 4932–4934.
25. Rodríguez-Manzo, J. A.; Wang, M. S.; Banhart, F.; Bando, Y.; Golberg, D. Multi-branched Junctions of Carbon Nanotubes *via* Cobalt Particles. *Adv. Mater.* **2009**, in press.
26. Johnson, D. J. Structure Property Relationships in Carbon-Fibers. *J. Phys. D* **1987**, *20*, 286–291.
27. Yu, M. F.; Lourie, O.; Dyer, M. J.; Moloni, K.; Kelly, T. F.; Ruoff, R. S. Strength and Breaking Mechanism of Multiwalled Carbon Nanotubes under Tensile Load. *Science* **2000**, *287*, 637–640.
28. Peng, B.; Locasio, M.; Zapol, P.; Li, S.; Mielke, S. L.; Schatz, G. C.; Espinosa, H. D. Measurements of Near-Ultimate Strength for Multiwalled Carbon Nanotubes and Irradiation-Induced Crosslinking Improvements. *Nat. Nanotechnol.* **2008**, *3*, 626–631.